Accepted Manuscript

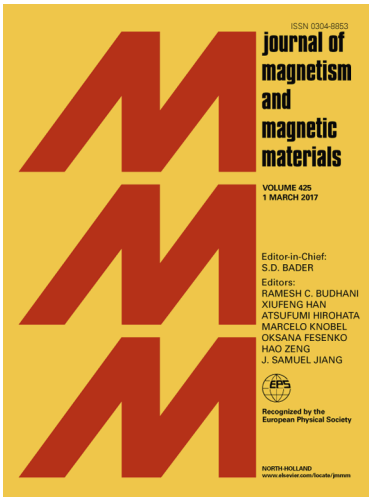

Research articles

Low temperature Mössbauer spectroscopic studies on Sm^{3+} doped Zn-Mn ferrites

V. Jagadeesha Angadi, S.P. Kubrin, D.A. Sarychev, Shidaling Matteppanavar, B. Rudraswamy, Hsiang-Lin Liu, K. Praveena

PII: S0304-8853(17)30053-7
DOI: http://dx.doi.org/10.1016/j.jmmm.2017.05.080
Reference: MAGMA 62784

To appear in: *Journal of Magnetism and Magnetic Materials*

Received Date: 6 January 2017
Revised Date: 30 March 2017
Accepted Date: 26 May 2017

Please cite this article as: V. Jagadeesha Angadi, S.P. Kubrin, D.A. Sarychev, S. Matteppanavar, B. Rudraswamy, H-L. Liu, K. Praveena, Low temperature Mössbauer spectroscopic studies on Sm^{3+} doped Zn-Mn ferrites, *Journal of Magnetism and Magnetic Materials* (2017), doi: http://dx.doi.org/10.1016/j.jmmm.2017.05.080

Low temperature Mössbauer spectroscopic studies on Sm^{3+} doped Zn-Mn ferrites

Jagadeesha Angadi V[1,2], S.P. Kubrin[3], D.A. Sarychev[3], Shidaling Matteppanavar[1], B.Rudraswamy[1], Hsiang-Lin Liu[4] and Praveena K[4*]

[1]Department of Physics, Bangalore University, Bangalore-560056, India
[2]Department of Physics, K.L.E.S's S.Nijalingappa College, Bangalore-560010, India
[3]Research Institute of Physics, Southern Federal University, Rostov-on-Don, Russia.
[4]Department of Physics, National Taiwan Normal University, Taipei-11677, Taiwan

Corresponding Authors: ***praveenaou@gmail.com***

Abstract: For the first time, we report on the low temperature Mössbauer spectroscopic study of $Zn^{2+}_{0.5}Mn^{2+}_{0.5}Sm^{3+}_{x}Fe^{3+}_{2-x}O_4$ (where x = 0.01-0.05) prepared by the modified solution combustion method using a mixture of urea and glucose as a fuel. The Mössbauer spectroscopy at room and low temperatures was applied to understand the magnetic properties of the samples. The room temperature Mössbauer spectroscopy results suggest that the occupation of the octahedral sites by Sm^{3+} ions leads to the distortion enhancement of ^{57}Fe nuclei environments, which leads to an increase in quadrupole splitting Δ values of D2 and D3 doublets. The low temperature Mössbauer spectroscopy results indicate that the presence of Sm^{3+} ions in the octahedron sites causes the decrease in the number of Fe – O – Fe chains. The transformation of Mössbauer spectra doublets into Zeeman sextets is accompanied by a significant decrease in the magnitude I_M of Mössbauer spectra intensity within the 0–1.2 mm/s velocity range normalized to its value at 300 K. This drop in the temperature dependence of I_M allows one to obtain the magnetic phase transition temperature T_N from the Mössbauer experiment.

Keywords: Zn-Mn ferrites; Zeeman sextets; Phase Transition; Low temperature Mössbauer spectroscopy.

1. Introduction

Recently, rare earth doped ferrite magnetic nanoparticle materials have been studied extensively due to their novel physics and chemical properties [1 – 4]. Among all materials, Lanthanum family (rare earth) doped ferrites are considered to be a group of technologically important materials that are used in electronics and in optoelectronics to manufacture magnetic, electronic and microwave devices, [5 – 7] permanent magnets, magnetic filters, transformers and magnetic switches owing to their high resistivity, negligible eddy current losses, high saturation magnetization and low coercivity. As such Lanthanum family (rare earth) doped ferrites are finding a large number of applications over a wide frequency range from a few kHz to several MHz. Zn-Mn ferrites are non-conductive [8] and ferromagnetic [9] however, the magnetic properties of Zn-Mn spinel ferrite depend on the interaction and cation distribution in the two sub-lattices of tetrahedral and octahedral sites. With the rapid development of mobile communication and information technology, small, inexpensive, and high performance electronic devices are in high demand. In this regard, we fabricated Sm^{3+} doped Zn-Mn ferrites by means of the solution combustion method using a mixture of fuels [10]. For the first time, we are reporting on the structural and low temperature Mössbauer spectroscopic properties of Sm^{3+} doped Zn-Mn ferrites and our results suggest that the synthesized materials can be helpful for high frequency applications.

2. Experimental

$Zn^{2+}_{0.5}Mn^{2+}_{0.5}Sm^{3+}_{x}Fe^{3+}_{2-x}O_4$ nanopowders were synthesized by the modified solution combustion method using stoichiometric amounts of $[Mn(NO_3)_2\ 4H_2O]^{2+}$, $[Zn(NO_3)_2\ 6H_2O]^{2+}$ $[Sm(NO_3)_3\ 9H_2O]^{3+}$ and $[Fe(NO3)_3\ 9H_2O]^{3+}$ as oxidizers and a mixture of fuels, *i.e* NH_2CONH_2 and $C_6H_{12}O_6$, as described earlier [11]. The precursors were dissolved in water. The combustion process was carried out inside a preheated muffle furnace. The solution was first boiled inside the furnace, then frothed and subsequently ignited. It took approximately 15-20 minutes for the

completion of the combustion process. The product was then grounded and characterized by XRD and HRTEM.

The XRD patterns of all the samples were recorded by a "PAN Analytical" X-ray diffractometer with Cu-Kα radiation in the 2θ range of 20-80° (step size: 0.02°). The high resolution transmission electron microscope (HRTEM) images were obtained with different magnification by the TITAN3TM 80-300 from FEI. The Mössbauer spectra were taken with the MS1104Em spectrometer designed and built in the Research Institute of Physics, Southern Federal University. The moving-source geometry was employed. The γ-ray source was ^{57}Co in a chromium matrix. The isomer shifts were calculated with respect to the metallic α-Fe. The samples were cooled in a helium cryostat CCS-850 (Janis Res. Inc., USA). The experimental spectra were fitted using SpectrRelax software [12].

3. Results and Discussion

3.1 Phase analysis

Fig. 1 presents XRD patterns of $Zn_{0.5}Mn_{0.5}Sm_xFe_{2-x}O_4$ (x = 0.01, 0.03 and 0.05) ferrite nanoparticles. The spectra show the characteristic reflections of a single phase cubic spinel structure and this indicates that the Sm^{3+} is incorporated into the spinel cubic lattice. However, a slight trace of Sm_2O_3 in addition to spinel phase is observed for x = 0.05, which can be explained by the lattice distortion due to the Sm^{3+} ion substitution. Ultimately, the internal stress caused by distortion leads to the formation of Sm_2O_3 in grain boundary. The (311) diffraction peak shows a slight shifting to a higher 2θ position, which is attributed to the increase of d-spacing resulting from the substitution of Sm^{3+} ions in the spinel cubic structure. The crystallite sizes were estimated using the Scherrer formula. These data are consistent with those of the particle sizes estimated by HRTEM, discussed earlier [11]. The XRD results reveal that an average crystallite size varies from 25 to 10 nm. There are two possible explanations to account for this decrease in crystallite size with an increase in Sm^{3+} concentration a) Firstly, the large size mismatch between Sm^{3+} and Fe^{3+} induces the crystalline anisotropy during the substitution of ions which creates the strain inside the volume of the crystals

with an increase in Sm^{3+} substitution. Furthermore, by balancing the crystal anisotropy and volume strain to each other the present system could remain in stable equilibrium. Therefore, the crystallite size decreases with an increase in Sm^{3+} substitution concentration in order to reduce the volume strain; b) Secondly, in the crystal structure of Sm^{3+} substituted Zn-Mn ferrite, $Zn^{2+,}$ and Mn^{2+} prefers tetrahedral (A-site) and octahedral (B-site) sites respectively. On the other hand, Fe^{3+} occupies either tetrahedral or octahedral site while Sm^{3+} ions have a tendency to enter into the octahedral site. However, it is difficult for Sm^{3+} ion to substitute Fe^{3+} as Sm^{3+} has much larger ionic radius than that of Fe^{3+} and requires more activation energy to enter octahedral sites as the bond energy of Sm-O is higher as compared to Fe-O. Therefore, instead of occupying the Fe^{3+} sites in the lattice the Sm^{3+} enter the lattice at interstitial sites due to extra stress coming from partial Sm^{3+} ion which suppresses the crystallite size [13]. The lattice parameter was found to increase from 8.420 to 8.445 Å with Sm^{3+} substitution, this is due to ionic radius of Sm (0.96 Å) bigger than the Fe (0.64 Å) which was reported about earlier [11]. It is considered that the substitution of Fe^{3+} sites by Sm^{3+} ones brings about the expansion of the unit cell, while preserving overall cubic symmetry with the increase in lattice parameter [10].

3.2 Particle Size analysis

We perform HRTEM measurements for the selected samples shown in Fig. 2(a-c). It can be seen that the particle sizes decrease with the increasing Sm^{3+} concentration ranges from 25 to 10 nm. The results are consistent with the trend in variation of particle sizes obtained from the XRD data. However, the observed differences in the absolute values of the average particle sizes could be result of the volume being occupied by bigger particles, although the number of such particles is small. This leads to sharper lines in the XRD but the average number of small particles is bigger than was observed by HRTEM. The selected area of electron diffraction patterns of the analyzed samples shows spotty circular ring patterns without any additional diffraction spots, which reveal their crystalline spinel cubic structure. These features indicate that the synthesized samples are of crystalline nature [11].

3.3 Mössbauer Spectroscopy Analysis

Fig. 3. shows the room temperature Mössbauer spectra of $Zn_{0.5}Mn_{0.5}Sm_xFe_{2-x}O_4$ (x = 0.01 - 0.05) nanoparticles. The spectra are broadened doublets with a slight asymmetry. The functions of the quadrupole splitting distributions were restored for each Mössbauer spectra. Each function has three local maxima with quadrupole splitting values $\Delta_1 \approx 0.40 \pm 0.02$ mm/s $\Delta_2 \approx 0.85 \pm 0.02$ mm/s and $\Delta_3 \approx 1.30 \pm 0.02$ mm/s. These values correspond to three paramagnetic the doublets with the parameters listed in Table 1. The isomer shift values of doublets are about ≈0.31 ± 0.35 mm/s and related to Fe^{3+} ions in oxygen octahedron [14]. The crystal inhomogeneity and superparamagnetic properties of the investigated nanoparticles are assumed to be responsible for the doublet lines broadening. Commonly the room temperature Mossbauer spectra consist of one symmetric paramagnetic doublet with parameters close to D2 [11, 15 – 17]. The presence of three doublets may be caused by the compositional disorder of Mn and Zn ions in tetrahedron states and the substitution of Fe^{3+} ions with Sm^{3+}. The cation disorder in tetrahedron state creates several types of iron containing octahedrons with different local distortions. This results in three doublets on Mössbauer spectrum. The doublet D1 with the lowest Δ value corresponds to the Fe^{3+} ion with most symmetrical environment. The doublets D2 and D3 correspond to the Fe^{3+} ions with different tetrahedrons in their surroundings. The occupation of the octahedral sites by Sm^{3+} ions leads to the distortion enhancement of ^{57}Fe nuclei environments, which provokes the increase in Δ values of D2 and D3 doublets.

Under low temperatures the Mössbauer spectra paramagnetic doublets of $Zn_{0.5}Mn_{0.5}Sm_xFe_{2-x}O_4$ (x = 0.01-0.05) nanoparticles transform into Zeeman sextets (Fig. 4). The magnetic field distribution functions of Mössbauer spectra taken at 15 K have three local maxima with $H_1 \approx 500$ kOe, $H_2 \approx 480$ kOe and $H_3 \approx 440$ kOe. These maxima correspond to three Zeeman sextets. The parameters of the sextets are listed in Table 2. The differences in H values of the sextets may associate with the compositional disorder of Mn and Zn ions in the tetrahedron sites. The sextet S1 with higher H value corresponds to the Fe^{3+} with symmetrical environment. The

presence of Sm^{3+} ions in the octahedron sites leads to the decrease in the number of Fe–O-Fe chains. The sextets S2 and S3 have lower H values because they have one and two Sm^{3+} ions in surrounding. The decrease in H values of S1 and S2 sextets with the growth of Sm^{3+} concentrations are also due to reducing number of Fe–O–Fe chains.

The transformation of Mössbauer spectra doublets into Zeeman sextets is accompanied by a significant decrease in the magnitude I_m of Mössbauer spectra intensity within the 0–1.2 mm/s velocity range normalized to its value at 300 K. This drop in the temperature dependence of I_m allows one to obtain the magnetic phase transition temperature T_M from the Mössbauer experiment. This method has been successfully applied for estimating T_M in perovskite-like compounds [18, 19]. Fig. 5 shows temperature dependence $I_m(T)$ - maximal intensity of the doublet of Mössbauer spectra of $Zn_{0.5}Mn_{0.5}Sm_xFe_{2-x}O_4$ (x = 0.01 - 0.05). The $I_m(T)$ value is slowly decreasing in the wide temperature range (250 – 50 K) due to the superparamagnetic properties of nanoparticles. Nevertheless, while x is growing, the slopes of I_m (T) dependencies tend to shift to the left, which indicates the decreasing in T_M value. This can be explained by the reducing number of Fe-O-Fe chains caused by the substitution of Fe^{+3} ions with Sm^{+3}.

The $I_m(T)$ dependence also helps to estimate the blocking temperature T_B. T_B is temperature when lines of Zeeman structure are resolved on Mössbauer spectra. Thus, when $T<T_B$, the Mossbauer spectroscopy measure time (t_m) is much shorter than superparamagnetic relaxation time (t_0). The T value where $I_m(T) \approx 0.5$ corresponds to T_B. The T_B allows the calculation of the magnetic anisotropy (K) using relation [20]:

$$T_B = \frac{aKV}{k}, \tag{1}$$

where $a = \frac{1}{\ln\left(\frac{t_m}{t_0}\right)}$, K is magnetic anisotropy, V is volume of the particle, k is Boltzmann's constant.

The calculated K values and estimated T_B values are present in Table 3. Generally, the K and T_B values are reduced with particle sizes decreasing [21]. However, the K value of the sample with $x = 0.5$ and average diameter ≈8 nm, is higher than for the sample with $x = 0.3$ and diameter ≈10 nm. This could be caused by the particles forming clusters.

4. Conclusions

The Sm^{3+} doped Zn-Mn ferrites were synthesized with the help of the modified solution combustion method using urea and glucose as a fuel. The effect of Sm^{3+} ion on the structure of the low temperature Mössbauer spectra were extensively studied for the first time. The X-ray diffraction pattern revealed that the synthesized samples exhibit a single phase with cubic spinel structure. The average crystallite size was found to decrease while the Sm^{3+} content increased. The obtained Mössbauer spectroscopy results suggest the existence of some local disorder in the arrangement of cations in the sub-lattice of all the analyzed samples. Furthermore, the low temperature Mössbauer spectroscopy results indicate that Sm^{3+} doping reduces the temperature of magnetic phase transitions and magnetic hyperfine field vales of Fe^{3+} ions. The reduction of particle sizes seem to lead to the decrease in blocking temperature and the formation of particle clusters.

Acknowledgements

The authors (JAV and BRS) are thankful to the UGC, New Delhi, for the financial support received through the Major Research project (File No.UGC-MRP-41-946). Dr K. Praveena acknowledges the Ministry of Science and Technology of Republic of China under Grant No. MOST 105-2112-M-003-013-MY3 and MOST 105-2811-M-003-018 for financial support.

References

[1] E. Ateia, M. A. Ahmed, A. K. El-Aziz, Effect of rare earth radius and concentration on the structural and transport properties of doped Mn-Zn ferrite, J. Magn. Magn. Mater. 311 (2007) 545-554.

[2] S. Thankachan, B. P. Jacob, S. Xavier, E. M. Mohammed, Effect of samarium substitution on structural and magnetic properties of magnesium ferrite nanoparticles, J. Magn. Magn. Mater. 348 (2013) 140-145.

[3] M. M. Rashad, R. M. Mohamed, H. El-Shall, Magnetic properties of nanocrystalline Sm-substituted $CoFe_2O_4$ synthesized by citrate precursor method, J. Magn. Magn. Mater.198 (2008)139-146.

[4] A. B. Gadkari, T. J. Shinde, P. N. Vasambekar, Structural analysis of Sm^{3+} doped nanocrystalline Mg-Cd ferrites prepared by oxalate co-precipitation method, Mater. Charact. 60 (2009) 1328-1333.

[5] J. Chand, S. Verma, M. Singh, Structural, magnetic and Mössbauer spectral studies of Sm^{3+} ions doped Mg ferrites synthesized by solid state reaction technique, J. Alloys Compd. 552 (2013) 264-268.

[6] E. Melagiriyappa, H. S. Jayanna., Structural and magnetic susceptibility studies of samarium substituted magnesium-zinc ferrites, J. Alloys Compd. 482 (2009) 147-150.

[7] V.J. Angadi, B. Rudraswamy, K. Sadhana, S. Ramana Murthy, K. Praveena, Effect of Sm^{3+}–Gd^{3+} on structural, electrical and magnetic properties of Mn–Zn ferrites synthesized via combustion route, J. Alloys Compd. 656 (2016) 5–12.

[8] J.A. Faria, *Electromagnetic foundations of electrical engineering*. Wiley, 2008.

[9] G.M. Joshi, V.R. Deo, S.N.Patil, Physics for Engineers, Ane Books India, 2008.

[10] V.J. Angadi, B. Rudraswamy, E. Melagiriyappa, Y. Shivaraj, S. Matteppanavar, Effect of Sm^{3+} substitution on structural and magnetic investigation of nano sized Mn–Sm–Zn ferrites, Indian J. Phys. 90 (2016) 881–885.

[11] V.J. Angadi, A.V. Anupama, R. Kumar, S. Matteppanavar, B. Rudraswamy, B. Sahoo, Observation of enhanced magnetic pinning in Sm^{3+} substituted nanocrystalline Mn–Zn ferrites prepared by propellant chemistry route, J. Alloys Compd. 682 (2016) 263–274.

[12] M. E. Matsnev and V. S. Rusakov. SpectrRelax: An Application for Mössbauer Spectra Modeling and Fitting. AIP Conf. Proc. 1489, 2012, 178-185.

[13] Vivek Chaudhari, Sagar E. Shirsath, M.L. Mane, R.H. Kadam, S.B. Shelke, D.R. Mane, Crystallographic, magnetic and electrical properties of $Ni_{0.5}Cu_{0.25}Zn_{0.25}La_xFe_{2-x}O_4$ nanoparticles fabricated by sol–gel method, J. Alloys Compd. 549 (2014) 213-220.

[14] F. Menil. Systematic Trends of the ^{57}Fe Mossbauer Isomer Shifts In (FeO_n) and (FeF_n) Polyhedra. Evidence of a New Correlation Between the Isomer Shift and the Inductive Effect of the Competing Bond T-X (*Fe) (Where X Is O or F and T Any Element with a Formal Positive Charge). J Phys. Chem. Solids 46 (1985) 763-789.

[15] Rashi Mathur, D.R. Sharma, S.R. Vadera, S.R. Gupta, B.B. Sharma, and N. Kumar. Room Temperature Synthesis of Nanocomposites of Mn-Zn Ferrites in A Polymer Matrix. NanoStructured Materials, 11 (1999) 677– 686.

[16] Z. Klencsár, Gy. Tolnai, L. Korecz, I.Sajó, P. Németh, J. Osán, S. Mészáros, E. Kuzmann. Cation distribution and related properties of $MnxZn_{1-x}Fe_2O_4$ spinel nanoparticles. Solid State Sciences 24 (2013) 90 –100.

[17] V.J. Angadi, A.V. Anupama, R. Kumar, H.M. Somashekarappa, K. Praveena, B. Rudraswamy, B. Sahoo, Evidence of structural damage in Sm and Gd co-doped Mn–Zn ferrite ceramics due to high-energy gamma irradiation, Ceramics International 42 (2016) 15933-15939.

[18] I. P. Raevski, S. P. Kubrin, S. I. Raevskaya, V. V. Stashenko, D. A. Sarychev, M. A. Malitskaya, I. N. Zakharchenko, V. G. Smotrakov, V. V. Eremkin. Dielectric and Mossbauer Studies of Perovskite Multiferroics. Ferroelectrics, 373 (2008) 121–126.

[19] I. P. Raevski, S. P. Kubrin, S. I. Raevskaya, V. V. Titov, D. A. Sarychev, M. A. Malitskaya, I. N. Zakharchenko, and S. A. Prosandeev. Experimental evidence of the crucial role of nonmagnetic Pb cations in the enhancement of the Néel temperature in perovskite $Pb_{1-x}Ba_xFe_{1/2}Nb_{1/2}O_3$, Phy. Rev.B 80 (2009) 024108.

[20] S. Mørup, H. Topsoe Mossbauer Studies of Thermal Excitations in Magnetically Ordered Microcrystals, Appl. Phys.11 (1976) 63-66.

[21] F. Gazeau, J.C. Bacri, F. Gendron, R. Perzynski, Yu.L. Raikher, V.I. Stepanov, E. Dubois. Magnetic resonance of ferrite nanoparticles: evidence of surface effects J. Magn. Magn. Mater. 186 (1998) 175—187.

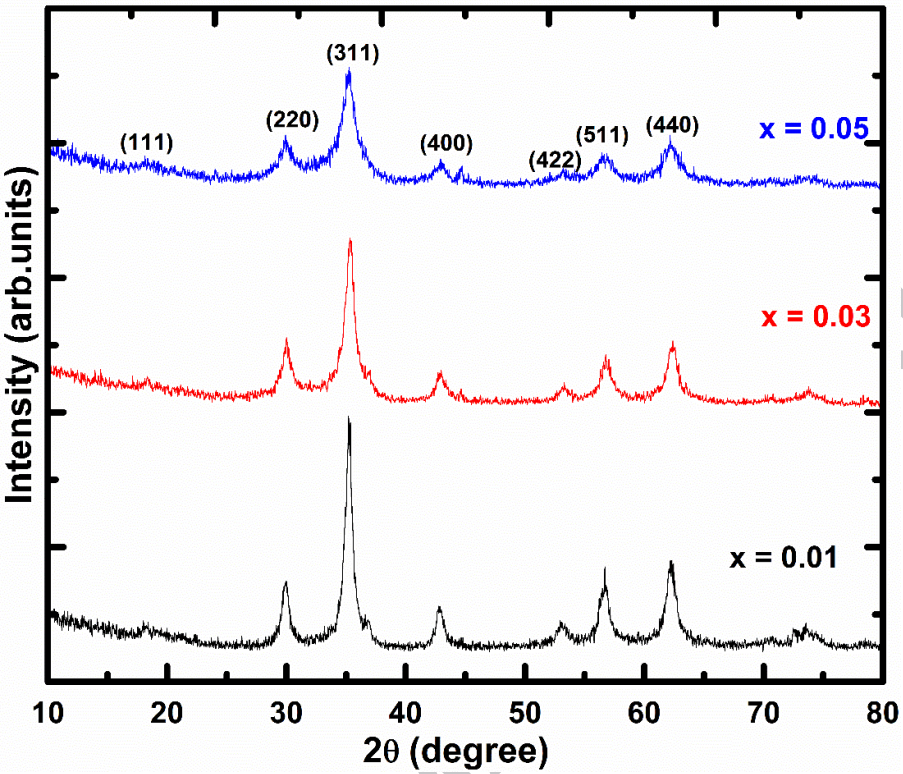

FIG. 1. Synthesized XRD patterns for $Zn_{0.5}Mn_{0.5}Sm_xFe_{2-x}O_4$ samples, where x = 0.01 0.03 and 0.05

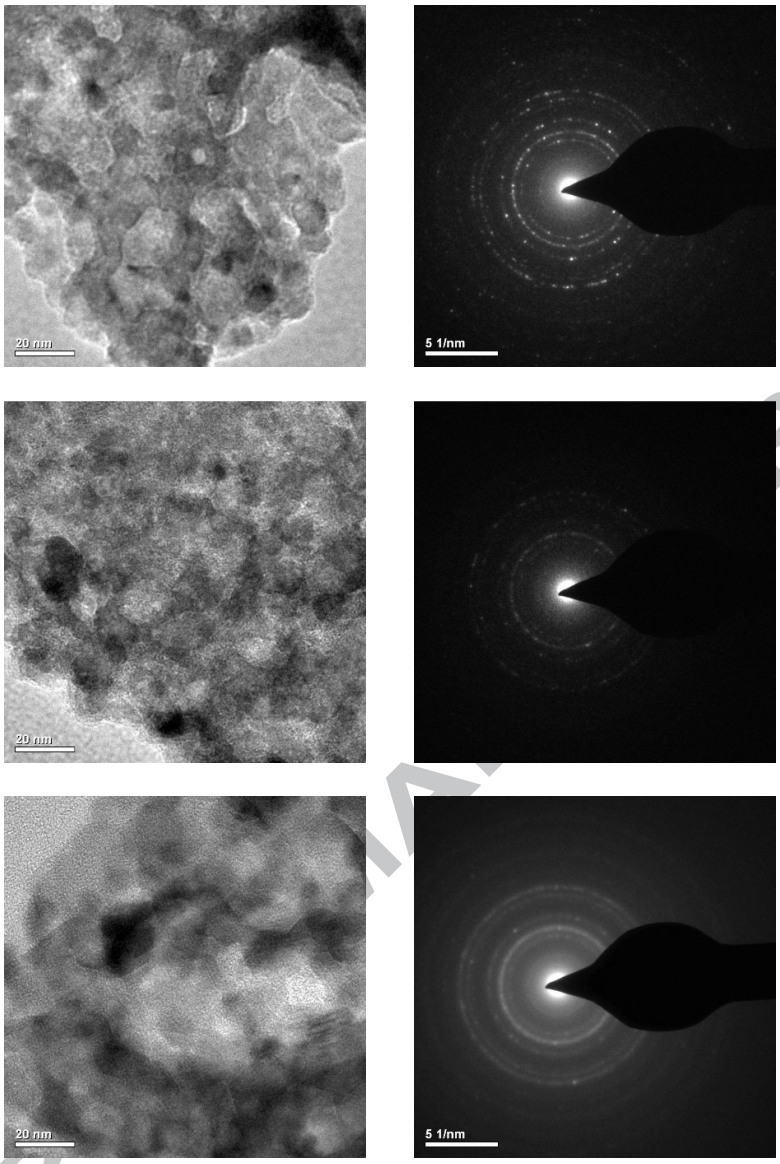

FIG. 2. HRTEM and SAED images for $Mn_{0.5}Zn_{0.5}Fe_{2-x}Sm_xO_4$ where x = 0.01, 0.03 and 0.05.

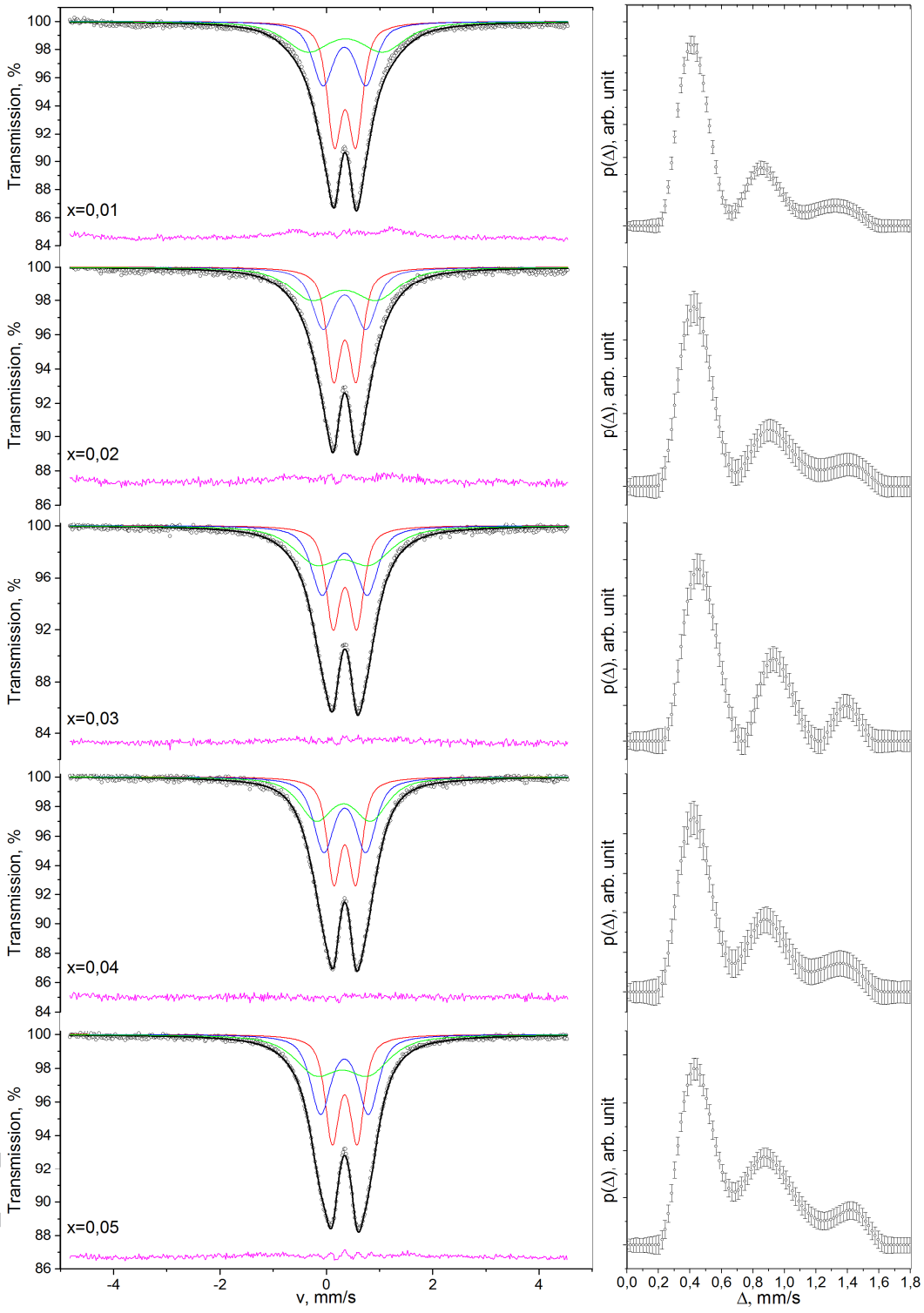

FIG. 3. Room temperature Mossbauer spectra of $Zn_{0.5}Mn_{0.5}Sm_xFe_{2-x}O_4$($x$=0.01—0.05) (left column) and reconstruction of the distribution functions of effective quadrupole splitting for the components of ^{57}Fe Mossbauer spectra (right column).

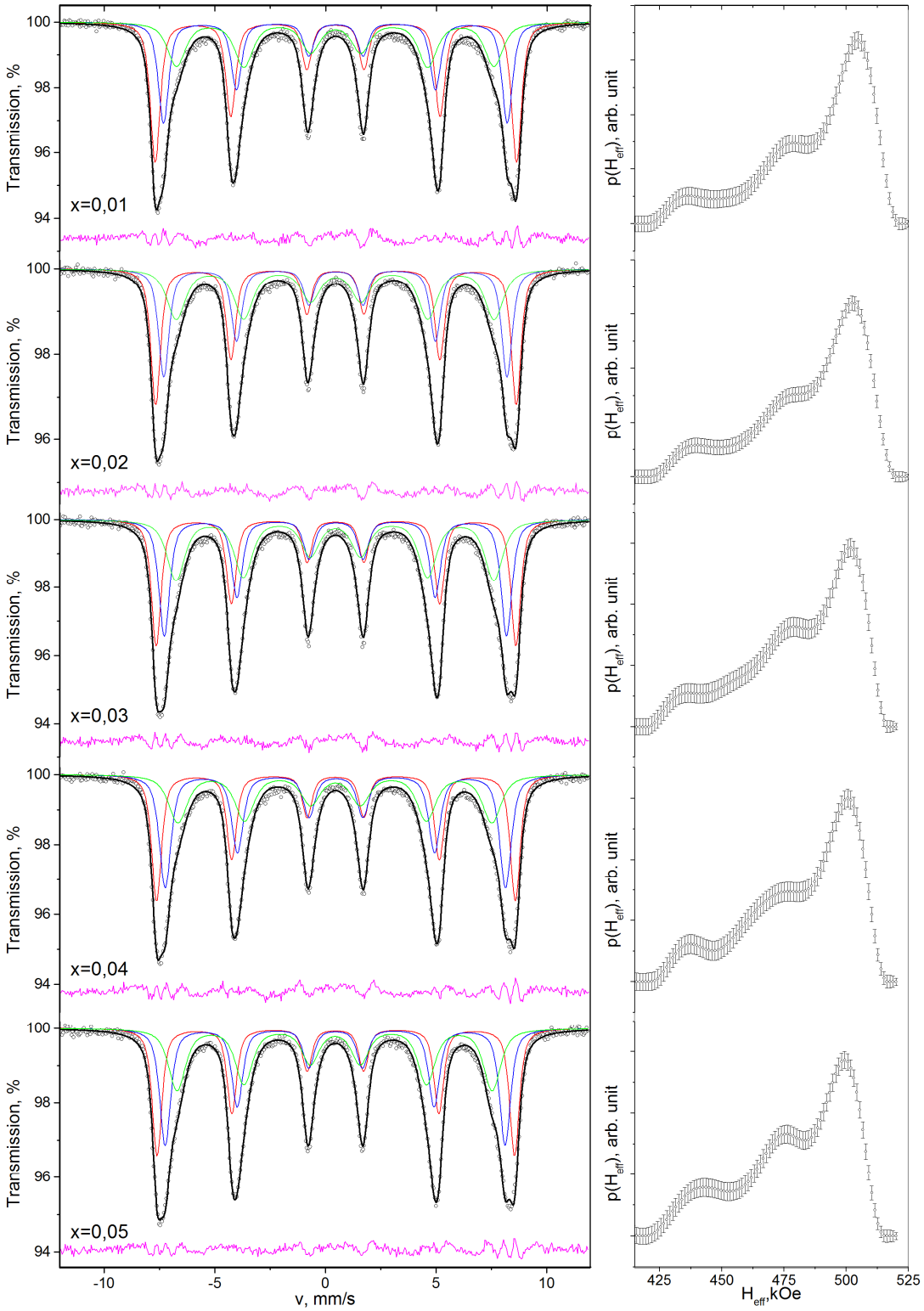

FIG. 4. Mossbauer spectra of $Zn_{0.5}Mn_{0.5}Sm_xFe_{2-x}O_4$($x$=0.01—0.05) taken at 15 K (left column) and reconstruction of the distribution functions of the effective magnetic field for the components of ^{57}Fe Mossbauer spectra (right column).

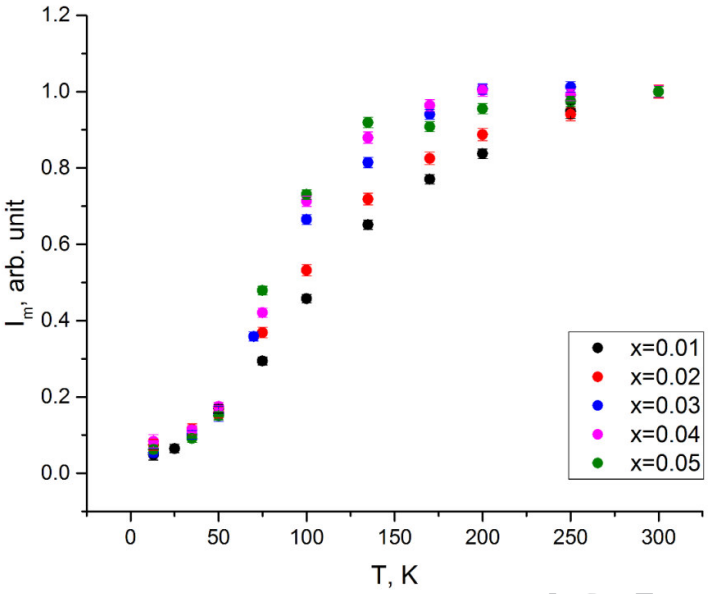

FIG. 5. Temperature dependences of I_m- maximal intensity of Mossbauer spectrum related to its value at 300 K for $Zn_{0.5}Mn_{0.5}Sm_xFe_{2-x}O_4$ (x = 0.01 – 0.05) samples.

Table 1. The parameters of room temperature Mossbauer spectra of $Zn_{0.5}Mn_{0.5}Sm_xFe_{2-x}O_4$ (x=0.01—0.05) δ — isomer shift, Δ — quadrupole splitting, A - component area, G – linewidth, χ^2 — Pearson's criterion.

x	Component	δ±0.02. mm/s	Δ±0.02. mm/s	A±2. %	G±0.02. mm/s	χ^2
0.01	D1	0.35	0.40	40	0.32	2.260
	D2	0.34	0.81	30	0.48	
	D3	0.31	1.38	30	1.00	
0.02	D1	0.34	0.42	36	0.32	1.950
	D2	0.34	0.80	31	0.49	
	D3	0.31	1.22	33	1.00	
0.03	D1	0.34	0.42	34	0.34	1.165
	D2	0.34	0.90	37	0.47	
	D3	0.33	1.39	29	1.00	
0.04	D1	0.34	0.40	33	0.32	1.046
	D2	0.34	0.90	35	0.45	
	D3	0.33	1.40	33	0.93	
0.05	D1	0.34	0.44	32	0.35	1.878
	D2	0.34	0.90	34	0.48	
	D3	0.32	1.42	34	1.03	

Table 2. The parameters of Mossbauer spectra of $Zn_{0.5}Mn_{0.5}Sm_xFe_{2-x}O_4$ (x=0.01—0.05) taken at 15 K. δ — isomer shift, ε – quadrupole shift, H_{eff} — effective magnetic field on ^{57}Fe, A - component area, G – linewidth, χ^2 — Pearson's criterion.

x	Component	δ±0.02. mm/s	ε±0.02. mm/s	H_{eff}±2. kOe	A±2. %	G±0.02. mm/s	χ^2
0.01	S1	0.45	0.02	506	40	0.53	3.231
	S2	0.45	-0.03	481	30	0.57	
	S3	0.43	-0.03	445	30	0.98	
0.02	S1	0.45	0.02	505	36	0.53	2.881
	S2	0.45	-0.03	481	31	0.57	
	S3	0.44	-0.03	445	33	1.00	
0.03	S1	0.46	0.03	504	32	0.52	3.327
	S2	0.46	-0.03	479	33	0.59	
	S3	0.43	-0.03	445	35	0.96	
0.04	S1	0.46	0.02	502	34	0.53	3.439
	S2	0.45	-0.03	476	36	0.63	
	S3	0.43	-0.03	440	31	1.01	
0.05	S1	0.46	0.02	501	32	0.52	2.874
	S2	0.46	-0.02	476	34	0.60	
	S3	0.43	-0.03	442	34	0.91	

Table 3. The values of average radius of nanoparticles r (HRTEM), blocking temperature T_B and magnetic anisotropy K of $Zn_{0.5}Mn_{0.5}Sm_xFe_{2-x}O_4$ samples

x	r, nm	$T_B \pm 5$, K	K, J/m^3
0.01	8	125	5.0×10^3
0.03	5	100	1.5×10^4
0.05	4	80	3.1×10^4

Graphical abstract

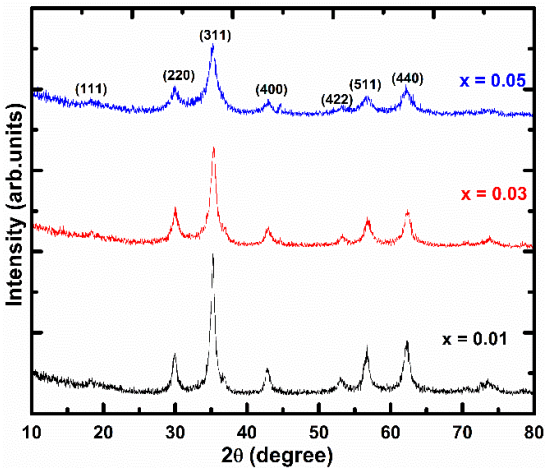

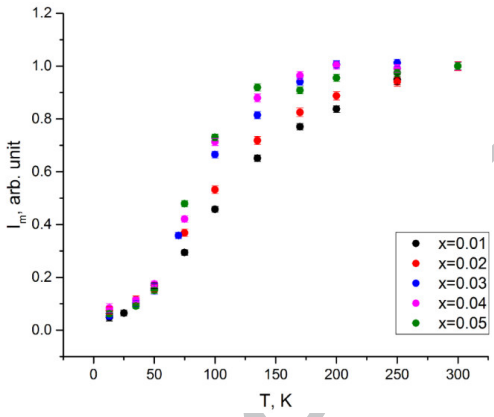

Highlights

- ✓ The average crystallite size from Scherrer formula is 25 nm.
- ✓ The RT Mössbauer spectroscopy results suggest the existence of some local disorder in the arrangement of cations in the sub-lattice.
- ✓ The low temperature Mössbauer spectroscopy results indicate that Sm^{3+} doping reduces the temperature of magnetic phase transitions and magnetic hyperfield vales of Fe^{3+} ions.